Advanced Receiver Tracking of Voyager 2 Near Solar Conjunction

D. H. Brown, W. J. Hurd, V. A. Vilnrotter, and J. D. Wiggins
Communications Systems Research Section

The Advanced Receiver (ARX) was used to track the Voyager 2 spacecraft at low Sun–Earth–probe (SEP) angles near solar conjunction in December of 1987. The received carrier signal exhibited strong fluctuations in both phase and amplitude. The ARX used spectral estimation and mathematical modeling of the phase and receiver noise processes to set an optimum carrier tracking bandwidth. This minimized the mean square phase error in tracking carrier phase and thus minimized the loss in the telemetry signal-to-noise ratio due to the carrier loop. Recovered symbol SNRs and errors in decoded engineering data for the ARX are compared with those for the current Block III telemetry stream. Optimum bandwidths are plotted against SEP angle. Measurements of the power spectral density of the solar phase and amplitude fluctuations are also given.

I. Introduction

It has long been known that strong solar corona effects can degrade the performance of telemetry systems. In particular, the solar corona causes variation in the phase of the received carrier [1], [2]. These effects are especially strong when the Sun–Earth–probe (SEP) angle is small. For optimum coherent receiver performance, these carrier phase variations should be tracked by the receiver. In a phase-locked loop receiver, this implies the use of a carrier loop bandwidth wide enough to track the phase variation. Unfortunately, loop bandwidths cannot be made arbitrarily large because the loop signal-to-noise ratio decreases with increasing loop bandwidth. This causes losses from phase jitter and cycle slipping at very low loop signal-to-noise ratios. For a given thermal noise spectral density (N_0), phase process spectral density, and carrier power, there is an optimum bandwidth which minimizes the total energy in the phase error signal and hence minimizes losses [3].

The Voyager 2 spacecraft, currently en route to its encounter with Neptune in 1989, passed within a 0.56-degree SEP angle on day of year (DOY) 359, December 25, 1987. This provided an opportunity to study solar effects and to evaluate a method for optimizing carrier tracking loop bandwidths developed for use with the DSN Advanced Receiver (ARX). The ARX is a digital receiver which performs carrier demodulation, subcarrier demodulation, and symbol synchronization in one integrated unit [4]. The optimization method was first used with the ARX during tracking experiments performed with the Pioneer 10 spacecraft in the spring of 1987 [5]. In these experiments, the aim was to quantify the phase process associated with the Pioneer 10 spacecraft oscillator. Since the Pioneer 10 signal level is nearing threshold, it is important that

it be tracked with the narrowest loop bandwidth possible. During these tests, phase processes much stronger than expected were observed. Investigation revealed this to be a solar effect, already significant for the weak Pioneer signal at an SEP angle of 11.8 degrees. This suggested that the method for optimizing loop bandwidth in the face of the fixed phase process associated with the Pioneer spacecraft oscillator could be applied to the time varying process of solar phase scintillation.

The ARX is well suited to this type of optimization. Since it implements its tracking loop filters digitally, filter bandwidths can be set with great accuracy and flexibility. Bandwidths available cover a range from approximately 0.05 to 100 Hz with better than 10 percent accuracy. The tracking bandwidth can also be changed in real time without dropping carrier lock. The measurement of the received carrier phase is facilitated by the fact that the ARX employs digital phase detection. The ARX records a sequence of outputs from its digital phase detector onto a floppy disk. An auxiliary computer then performs spectrum analysis on these records in near-real time and, from this, estimates the phase process spectral density and thermal noise level, and then the optimum tracking loop bandwidth. In the future, the spectrum analysis and bandwidth optimization will be performed in the ARX in real time.

The main goal of this experiment was to demonstrate the telemetry performance of the ARX with near-real-time bandwidth optimization and to compare it with the current receiver chain in the presence of strong solar corona effects. Additionally, we hoped to gain a better understanding of solar corona effects and of the behavior of digital phase-locked loops in this type of environment.

II. Experiment Description

The experiment involved tracking the Voyager 2 spacecraft at decreasing SEP angles with the ARX and the standard station configuration, and decoding and evaluating the two recovered telemetry streams. The success criterion for the experiment was that the decoded data from the ARX data stream have a comparable number of errors or fewer errors than the standard station. This allowed for a good relative performance measure, independent of SNR estimators which could be affected by amplitude variation.

The ARX provides improved performance by using the near-real-time bandwidth optimization technique as described above. As the system noise temperature and the magnitude of the phase process increase, the optimization algorithm computes new bandwidths and keeps the losses minimized. Operationally in the DSN, using the Block III receiver, the strategy for dealing with the solar effects is to use a wide loop bandwidth to track the phase perturbations. With low or highly variable signal levels, this approach can lead to losses from excessive carrier phase jitter. It should be emphasized, however, that at very low SEP angles, the introduction of amplitude variation makes this a highly complex tracking environment. For example, some instances may occur where the amplitude fading is so severe that no phase-locked loop could maintain lock. In such a case, wide bandwidths may be more desirable in terms of reacquisition.

A. Experiment Configuration

The experiment configuration used is shown in Fig. 1. All tracks in this experiment were done on the 34-meter high efficiency antenna at Goldstone (DSS-15). The lower path in Fig. 1 shows the standard station configuration. The standard configuration uses a Block III receiver, a Subcarrier Demodulator Assembly (SDA), and a Symbol Synchronizer Assembly (SSA). The output of the SSA is a stream of soft-quantized symbols which is sent to a Maximum Likelihood Convolutional Decoder (MCD). The MCD outputs bits to a Telemetry Processor Assembly (TPA) which sends the data back to JPL via the ground communications facility (GCF). Backup tapes are also made at the station.

At the minimum SEP angle, the Block III tracked with a nominal two-sided threshold bandwidth of 48 Hz, $2B_{L_0}$. Operating at +15 dB above threshold, this translates into an actual one-sided loop bandwidth of B_L = 70 Hz. The SDA was configured with a medium loop bandwidth which is a nominal 0.375 Hz. The SSA was configured for the medium range, narrow subrange, which at this symbol rate yields a loop bandwidth of 0.4 Hz.

The ARX used an independent parallel channel shown as the upper branch in Fig. 1. The VLBI downconverter mixes the low noise amplifier output against 8100 MHz. At the nominal Voyager 2 carrier frequency of 8420 MHz, this centers the frequency band of interest at 320 MHz. This is then mixed against 267 MHz to produce a carrier near 53 MHz, which is the center of the ARX tracking range. The receiver tracks carrier, subcarrier, and symbol phases and produces soft symbols directly. These are then passed to an MCD for decoding.

ARX carrier tracking loop bandwidths are selected as indicated by the near-real-time optimization algorithm. The subcarrier and symbol tracking loops in the ARX for all test cases used the following parameters. Both subcarrier and symbol loop bandwidths were set to 0.1 Hz, and both used type III loops. Initial acquisition was performed with 1.0-Hz type II loops. These were then narrowed in two steps.

B. Spectral Estimation and Bandwidth Optimization Method

Phase error spectra were obtained by performing Fourier analysis on the digital phase detector output. The phase detector outputs, which are passed to the software for filtering, were recorded onto a floppy disk. Each output file so generated contained M records of N points per record collected at a rate of r points per second. The recording rate determines the total bandwidth of the transform. The number of points determines the resolution of the transform.

The output was processed on a Compaq 286 portable microcomputer. Each record was Fourier transformed using the FFT algorithm. Then the resulting spectra were averaged across the M records to provide a less noisy estimate of the received spectrum. The averaged spectra were then processed with the "ad hoc" estimator as described in [3]. This produced estimates of σ_n^2 and σ_p^2, which are estimates of the contribution of thermal noise and phase process, respectively, to total phase error variance. Estimates of optimum bandwidth were produced from these variances and from knowledge of the tracking filter parameters. These values were also used as seed values for a maximum likelihood estimator which produced more accurate estimates of the noise parameters in post-processing [6].

III. Results

The ARX tracked the Voyager 2 spacecraft from DSS-15 on DOYs 345, 348, 354, 355, 356, 357, and 358 of 1987. In this section, we present the performance comparison results in terms of recovered SSNR and errors in decoded engineering data. Also presented is a record of the solar effects and their impact in terms of phase distortion, thermal noise temperature, and amplitude variation as a function of SEP angle. These data are then tied together into a practical form in a plot of optimum carrier tracking bandwidth vs. SEP angle.

A. Recovered Symbol SNR

Figures 2 and 3 show the recovered symbol SNR for the two streams as a function of time for DOYs 357 and 358. For all previous days, the solar effects were not significant enough to degrade the recovered SSNR.

By DOY 357 (Fig. 2), with an SEP angle of 2 degrees, the solar effect is becoming significant in both carrier phase and amplitude (see Section IIIB). The SSNR measured by the standard station telemetry string is 3 to 4 dB less than that of the ARX and of its own measurement for DOY 345. The increase in system noise temperature for this day relative to DOY 345 was only two degrees. One possible explanation for this discrepancy is that the varying amplitude has a strong biasing effect on the SSA SNR estimator. The SSA uses the moment method of SNR estimation. This produces a biased estimate which is then unbiased by the TPA. The moment method uses the square of the mean symbol value, as opposed to the mean of the symbol value squared, to estimate the mean squared. With a varying mean, the former approach will always yield a lower estimate of the mean squared than the latter and hence a lower estimate of SNR. The split symbol SNR estimator used in the ARX computes the mean of the squared symbol value and hence always measures the true average SNR, even when it is time varying. Since all data were decoded without error in both the ARX and standard telemetry streams, it is not known whether there actually was significant degradation in the standard string or whether there was merely inaccuracy in the SSA SNR estimator.

This effect can be seen again for the SNR plots of DOY 358 (Fig. 3). The SNR estimates for the standard station configuration are very low compared with the estimates for the ARX. Based on the standard station estimate of P_c/N_0 and the knowledge of the modulation index and symbol rate, values in the range of 7 to 8 dB were expected. The ARX estimates are in this range. These are also consistent with the 2.4-dB increase in system noise temperature predicted.

B. Comparison of Decoded Data

The only day on which significant error rates were expected was DOY 358. Unfortunately, on this day, a failure in the station air-conditioning system caused the data recording equipment to fail at the start of the pass and the entire station to be down for several hours. Thus for a majority of the day there is no recorded telemetry. Service was restored toward the end of the pass, in time to provide about 40 minutes of data for comparison.

Due to the regular nature of the engineering data being transmitted at the time, it was easy to identify errors once the data were decoded. The data were processed and analyzed by members of the Voyager project team. As expected, data from DOY 357 were error-free for both receivers. The data on DOY 358, however, indicated solar degradation effects on both data streams. On ten spacecraft engineering channels, a total of 27 errors were found in the standard station receiver data and 24 were found in the ARX data. How these errors relate to receiver performance is unclear. Nine of these errors were concurrent errors; that is, both data streams produced errors for that data point. These errors were probably the result of strong fades in the signal strength at those points. In addition, each data point is made up of 8 bits which are derived from the symbol stream via the rate 1/2 decoder. Thus we are not able to determine what the symbol error was at the output of either receiver based on the engineering data quality. What can

be said is that the ARX performed at least as well as the current system in terms of recovered data.

C. Solar Effects

In these experiments the ARX was shown to be an excellent tool for measuring solar effects. The power spectral densities of both phase and amplitude fluctuations obey inverse power relations in certain regions around the carrier frequency of the form

$$S(f) \approx S_1 f^{-\alpha}$$

The exponent α for the case of solar scintillation at low SEP angles is typically 8/3 or less [2]. The parameter S_1 is commonly interpreted as the value of the phase process power spectral density at 1 Hz. For a given α, S_1 indicates the strength of the disturbance. In this section we plot S_1, P_c/N_0, and optimum bandwidth as functions of SEP angle.

1. **S_1 vs. SEP.** Much new work has been done recently in using the ARX to estimate solar scintillation parameters. The data below were produced by using the "ad hoc" estimator introduced in [3]. Although this method may have unmodeled error sources, it does produce reasonable values for use in estimating optimum carrier bandwidth, and was used in our field experiments. Figure 4 shows a plot of S_1 vs. SEP angle for angles from 0.86 to 4.6 degrees. Note the sharp increase in S_1 under a 2-degree SEP angle.

2. **P_c/N_0 vs. SEP.** Figure 5 shows a plot of P_c/N_0 vs. SEP. The values below 2 degrees are lower than expected, possibly due to amplitude fluctuations biasing the estimator as in the SNR estimator in the SSA. The ARX estimates its received carrier power by averaging the in-phase channel samples and then squaring the average, which as mentioned before produces a value which is biased down. This effect could have been avoided by averaging over shorter periods such that the amplitude was constant in that period.

3. **Optimum bandwidth vs. SEP.** One of the important products of this work is that we now have a better idea of what loop bandwidth can be used when solar phase and amplitude scintillation are significant. The plot of optimum bandwidth vs. SEP as determined by the ARX is given in Fig. 6. These values should apply for any phase-locked loop whose minimum loop bandwidth is limited by solar phase scintillation. Specifically, this implies that the Block III could have tracked to within a 1-degree SEP angle with a two-sided loop bandwidth $2B_{L_0}$ = 12 Hz loop and increased the tracking margin by 6 dB.

4. **Amplitude scintillation.** The analysis of solar effects is significantly complicated by variation in amplitude. The loop parameters, which affect the spectrum of the phase detector output, are not constant in this case. Several approaches are being developed [6] to deal with these effects, including real-time adaptive techniques to modify the loop filter coefficients in response to changing signal levels. To indicate the level of amplitude variation, Figs. 7, 8, and 9 show raw in-phase channel samples as a function of time for DOYs 345, 356, and 358, which correspond to SEP angles of 11 degrees, 2.5 degrees, and 0.9 degree, respectively.

On DOY 345, solar effects are negligible, and the fast variations in Fig. 7 are due to errors in measuring carrier amplitude due to receiver noise. Significant slow variations in carrier amplitude are evident in DOYs 356 and 358. These slow variations are due to solar scintillation. On DOY 358, with an SEP angle of 0.9 degree, the estimate of carrier amplitude actually goes negative at times. This appears to be due to very deep amplitude fades and the resulting cycle slipping in the carrier loop.

IV. Conclusions

The Advanced Receiver was demonstrated successfully with the Voyager 2 spacecraft near solar conjunction. Using much narrower bandwidths, the ARX demonstrated performance equal to or better than that of the current station configuration in terms of the quality of the decoded data. By using near-real time bandwidth optimization, it was demonstrated that narrower bandwidths could be used at solar conjunction, thus increasing threshold by as much as 6 dB when solar phase scintillation dominates the received carrier phase process. Comparison of recovered SNR is not applicable due to the inaccuracy of the standard station estimators in an amplitude fluctuating environment.

References

[1] J. W. Armstrong, R. Woo, and F. B. Estabrook, "Interplanetary Phase Scintillation and the Search for Very Low Frequency Gravitational Radiation," *Astrophysical Journal*, vol. 230, p. 570, June 1, 1979.

[2] R. Woo and J. W. Armstrong, "Spacecraft Radio Scattering Observations of the Power Spectrum of Electron Density Fluctuations in the Solar Wind," *Journal of Geophysical Research*, vol. 84, no. A12, pp. 7288–7296, December 1, 1979.

[3] V. A. Vilnrotter, W. J. Hurd, and D. H. Brown, "Optimized Tracking of RF Carriers With Phase Noise, Including Pioneer 10 Results," *TDA Progress Report 42-91*, vol. July–September 1987, Jet Propulsion Laboratory, Pasadena, California, pp. 141–157, November 15, 1987.

[4] D. H. Brown and W. J. Hurd, "DSN Advanced Receiver: Breadboard Description and Test Results," *TDA Progress Report 42-89*, vol. January–March 1987, Jet Propulsion Laboratory, Pasadena, California, pp. 48–66, May 15, 1987.

[5] W. J. Hurd, D. H. Brown, V. A. Vilnrotter, and J. D. Wiggins, "Telemetry SNR Improvement Using the DSN Advanced Receiver, With Results for Pioneer 10," *TDA Progress Report 42-93*, vol. January–March 1988, Jet Propulsion Laboratory, Pasadena, California, May 15, 1988 (this issue).

[6] V. A. Vilnrotter, D. H. Brown, and W. J. Hurd, "Spectral Estimation of Received Phase in the Presence of Amplitude Scintillation," *TDA Progress Report 42-93*, vol. January–March 1988, Jet Propulsion Laboratory, Pasadena, California, May 15, 1988 (this issue).

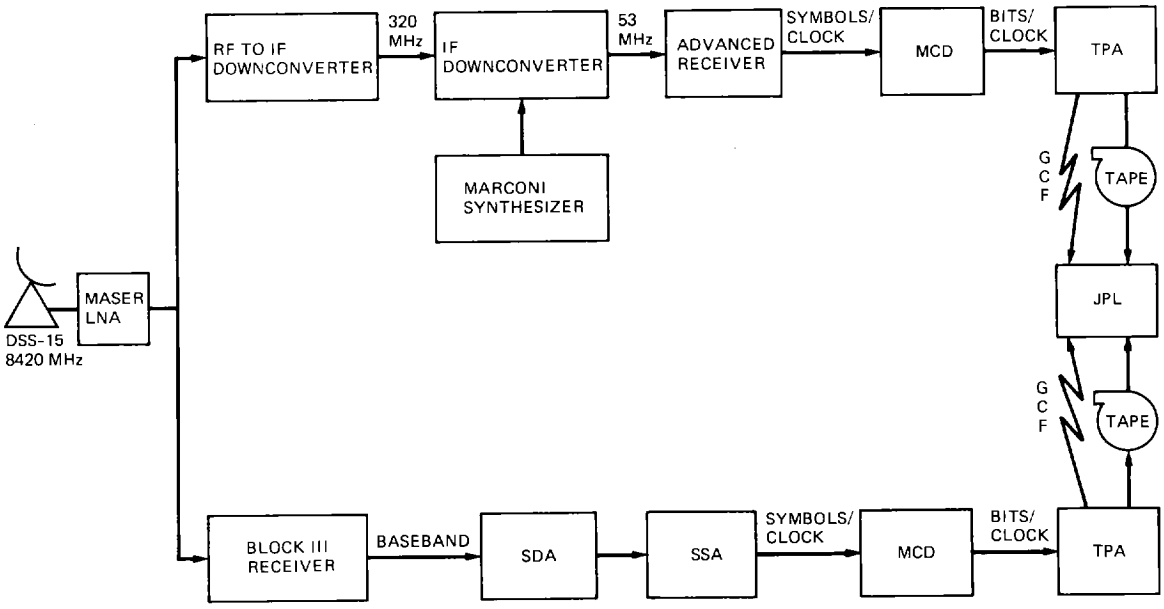

Fig. 1. Configuration for the solar conjunction experiment

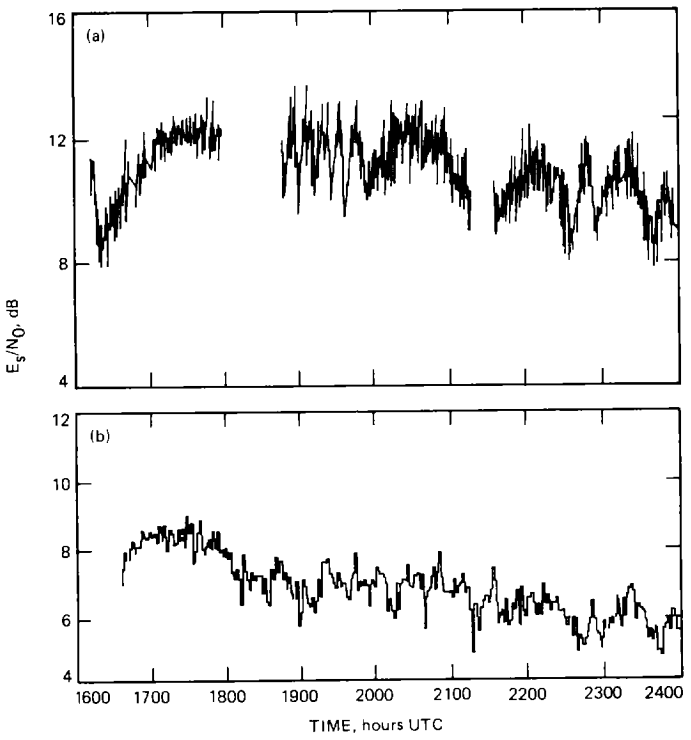

Fig. 2. DOY 357: (a) ARX SSNR vs. time; (b) station SSNR vs. time

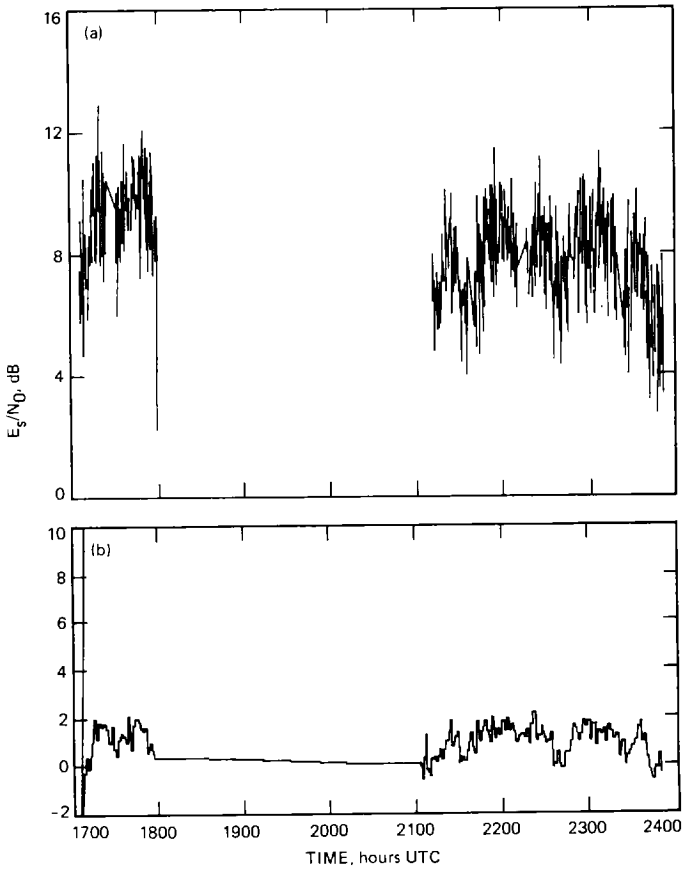

Fig. 3. DOY 358: (a) ARX SSNR vs. time; (b) station SSNR vs. time

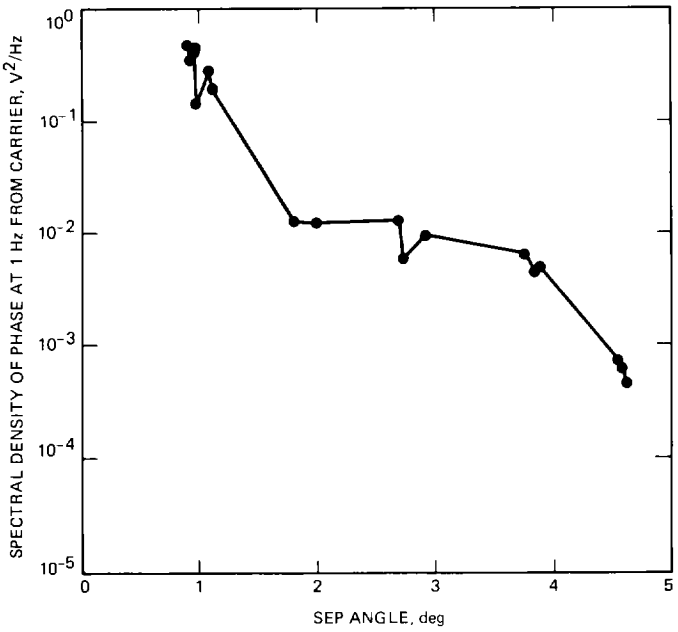

Fig. 4. Spectral density vs. SEP angle

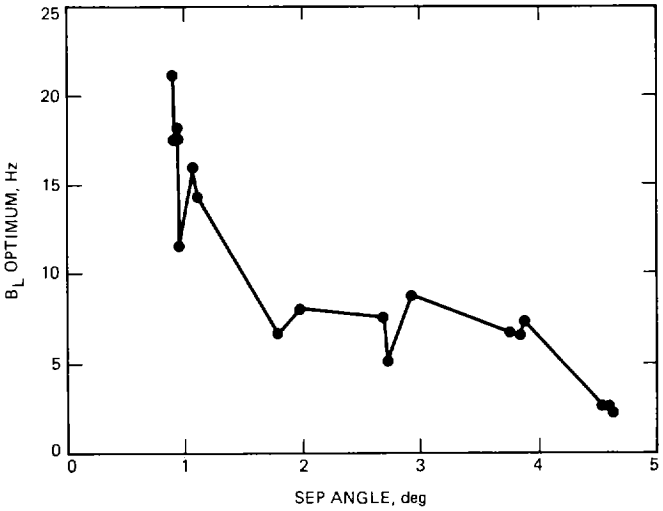

Fig. 6. Optimum carrier loop bandwidth

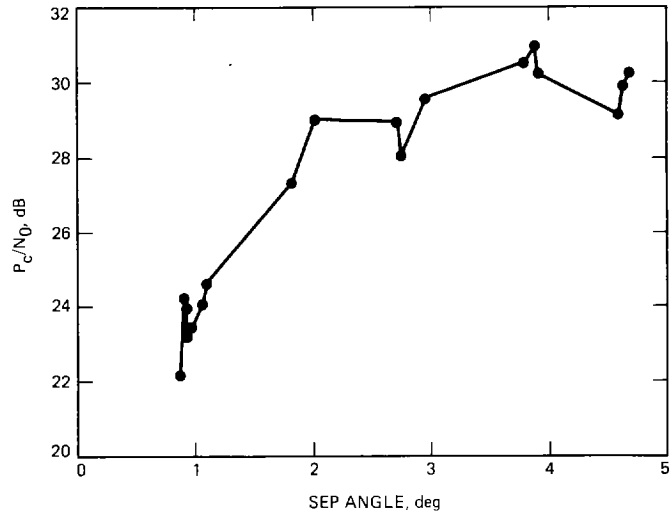

Fig. 5. P_c/N_0 vs. SEP angle

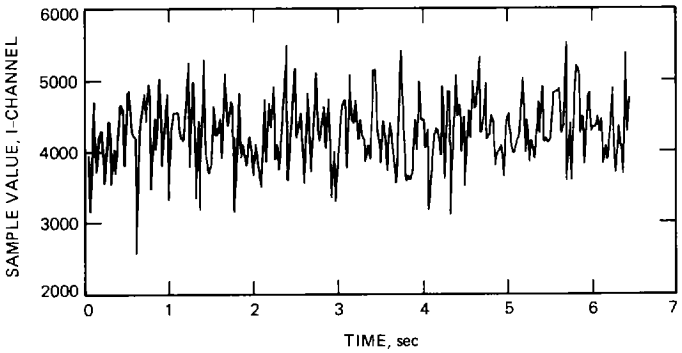

Fig. 7. In-phase channel sample values vs. time: DOY 345

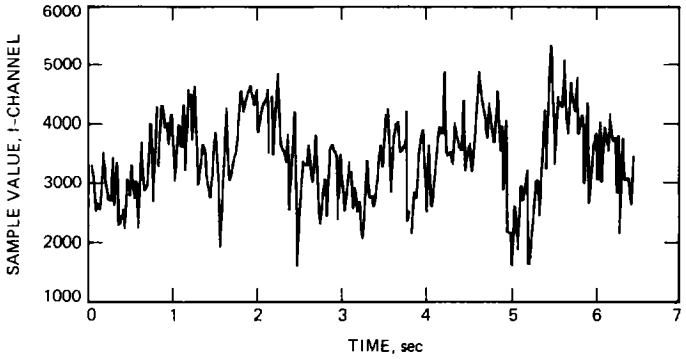

Fig. 8. In-phase channel sample values vs. time: DOY 356

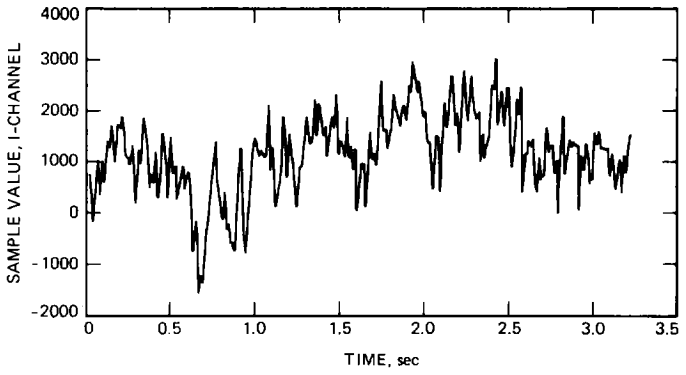

Fig. 9. In-phase channel sample values vs. time: DOY 358